An Observer Looks at the Temperature in the 3WCC

A. Simon*,**, D. Nelson-Gruel*, S. Onori***, A. Charlet*, T. Jaine**, G. Colin*, C. Nouillant**, Y. Chamaillard*

*Laboratoire PRISME - Université d'Orléans,
8 rue Léonard de Vinci, 45072 Orléans, France (e-mail: dominique.gruel-nelson@univ-orleans.fr).
** Groupe PSA, Direction Research Innovation & Advanced Technologies, 92250 La Garenne-Colombes, France
*** Department of Automotive Engineering - Clemson University, Greenville, SC 29607 USA

European standards on pollutants have resulted in the systematic integration of a three-way catalytic converter (3WCC) on gasoline engines. The conversion efficiency of the 3WCC is strongly dependent on the temperature of the 3WCC itself. Knowing this temperature is a key element in predicting and minimizing the real quantities of pollutants that the gasoline engine rejects. Due to cost issues, it is really difficult to obtain this information through a direct measurement. This article presents a complete methodology for estimating exhaust gas and catalyst temperature in real time. The first step of this methodology consists of building a 1-dimensional physical model (1D model) of the 3WCC's temperature. All of the parameters of this model are identified using some experimental data and a particle swarm optimization algorithm. The second step of the proposed methodology consists of using an extended Kalman filter algorithm to estimate all temperatures in real time from a linearized model based on the previous 1D physical model and a measurement downstream of the 3WCC. Every step of this methodology is validated using experimental data.

Keywords: Observer, Extended Kalman Filter, thermal model, three-way catalytic converter, after-treatment systems

1. INTRODUCTION

To reduce pollutant emissions and improve the performance of the vehicle, the development of a more efficient after-treatment system is needed. For most of the after-treatment systems applied in the automotive industry, their efficiency is strongly dependent on its internal temperature as shown in fig. 1. Therefore, if we consider a gasoline Hybrid Electric Vehicle (HEV), one key issue consists of searching for the best way to warm up and maintain its after-treatment systems, the 3-Way Catalytic Converter (3WCC), at high temperature with constraints on pollutant emissions and consumption as shown in Michel et al. (2017). Indeed, hybridization of a vehicle appears to be a good alternative to lowering CO_2 and pollutant emissions. However, hybridization can lead to a period of time where the thermal engine is not used, and it is impossible to maintain locally or globally the 3WCC at a sufficiently high temperature to be able to convert the pollutants. Therefore, being able to determine the temperature of the 3WCC can be useful in order to be aware in real-time of the amount of pollutants effectively converted and to establish an on-line strategy for a hybrid vehicle like in Simon et al. (2015).

Some research was done in modelling the temperature of the 3WCC. Brandt et al. (2000) and Cioffi et al. (2001) developed a control-oriented model that can be easily implemented on an ECU. However, those models are not accurate enough during the warm-up phase. Bresch-Pietri et al. (2013) presented a reduced 1-D input delay models that improve the light-off prediction but without a physical approach. Sabatini et al. (2015) developed a simplified 1-D

physical model based on the work of Auckenthaler et al. (2005). The simplification consists of expressing the exothermic reaction as a function of the exhaust mass flow and a global conversion rate. With a similar approach, Michel et al. (2014) considered the mass flow of three pollutants (CO, HC and NO_X) and gave a conversion rate for each one of them so the exothermic reaction could be representative of the air to fuel ratio and the operating point. Using a different approach, Utz et al. (2014) suggests a catalytic converter temperature observer using an Extended Kalman Filter (EKF) and a measurement inside the 3WCC to correct the error of the thermal model.

This paper presents two improvements on the previous work. First, in order to model the impact of hybridization on the global efficiency of the 3WCC, it is necessary to consider local conversions of pollutants. Using the models of Sabatini et al. (2015) and Michel et al. (2014), we have added a spatial variation of pollutants to calculate the exothermic reaction and the output emissions as function of local conversions. This model is presented in the part two of this paper, while the identification of its parameters with experimental data is detailed in part three.

Second, to ease the physical implementation of an estimator like Utz et al. (2014), a temperature observer with a measurement outside of the 3WCC is proposed. The design, implementation and results of the EKF that estimate the internal 3WCC temperatures is explained in part four. The validation of this observer is also supported with experimental data. Finally, this article is concluded in part five and completed with some perspectives regarding this work.
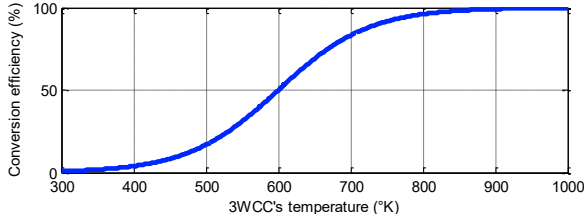
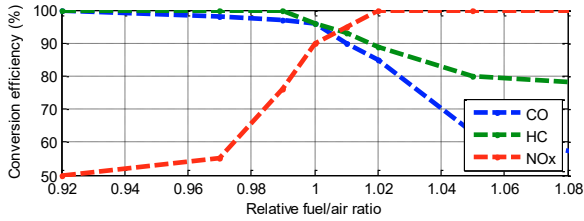Fig. 1: Impact of the temperature on the conversion efficiency.

Fig. 2: Impact of the relative fuel/air ratio on the conversion efficiency.

2.   THREE-WAY CATALYTIC CONVERTER

2.1. Overview

The 3WCC converts the pollutants emitted by the gasoline engine into less harmful emissions. The catalytic converter used for this work is composed of a ceramic brick as a substrate, sprayed with a washcoat of Alumina Oxide (Al_2O_3) containing noble metals such as Palladium (Pd), Platinum (Pt) and Rhodium (Rh). These noble metals give the 3WCC the ability to convert a fraction of the pollutant emissions such as carbon monoxide (CO), unburned hydrocarbons (HC) and nitrogen oxides (NO_X) to carbon dioxide (CO_2), water (H_2O), and nitrogen (N_2) through catalytic oxidation and reduction. However, two conditions need to be fulfilled to obtain a good conversion efficiency: a high catalyst temperature (Fig. 1) and a stoichiometric fuel to air ratio in the exhaust gas (Fig. 2).

2.2. Thermal model of 3WCC

In order to predict the thermal behaviour of the cylindrical 3WCC during warm-up and hybrid powertrain conditions, a 1-D physical thermal model along its axe is chosen. Indeed, the axial thermal gradient in a 3WCC can be important because of its high thermal inertia and its low thermal conductivity. Looking at the case of a cylindrical 3WCC, the radial thermal gradient is not taken into account with the hypothesis of a well-sprayed exhaust mass flow on the input surface. To ally a physical and simplified approach, the model used in this paper is from Sabatini et al. (2015). It consists of a two-phases gas/solid energy balance model. The exhaust gas is represented by the gas phase:

$$\rho_g \; \varepsilon \; C_{p,g} \frac{\partial T_g(x,t)}{\partial t} = -\frac{\dot{m}_{exh}(t)}{A_{cs}} C_{p,g} \frac{\partial T_g(x,t)}{\partial x}$$
$$+\varepsilon \; \lambda_g \frac{\partial^2 T_g(x,t)}{\partial x^2} + h_{int,cat} \; A_{geo} \left(T_{cat}(x,t) - T_g(x,t) \right). \tag{1}$$

Table 1. Nomenclature

Parameter	Description	Unit
ρ	Density	kg/m^3
ε	Volume fraction of the gas phase	-
C	Specific heat capacity	J/(K.kg)
λ	Heat conductivity	W/(K.m)
$\dot{m}_{exh}$	Exhaust mass flow	kg/s
A_{cs}	Catalyst cross section	m^2
$h_{int,cat}$	Convection 3WCC/gas	W/(K.m^2)
A_{geo}	Specific geometric catalyst surface	m^2/m^3
A_{out}	External surface of the 3WCC	m^2
V_{cat}	Volume of the 3WCC	m^3
$h_{ext,cat}$	Convection 3WCC/ambient	W/(K.m^2)
$K_{i,react}$	Exothermic coefficient	J/kg
$\dot{m}_i$	pollutant mass flow	kg/s
$\eta_{i,conv}$	Efficiency of conversion	-
L_{cat}	Length of the 3WCC	m
$T_{i,LO}$	Light-off temperature	K
s_i	Slope of the conversion's efficiency function	K^{-1}
$h_{int,post}$	Convection post/gas	W/(K.m^2)
$h_{ext,post}$	Convection post/ambient	W/(K.m^2)

The evolution of the gas temperature depends respectively on the axial enthalpy transfer, the heat conduction of the gas and the convective exchange between the gas and the solid.

The catalytic converter is considered as the solid phase of the model and its thermal behaviour is described by:

$$\rho_{cat}(1-\varepsilon)C_{cat} \frac{\partial T_{cat}(x,t)}{\partial t} = (1-\varepsilon)\lambda_{cat} \frac{\partial^2 T_{cat}(x,t)}{\partial x^2}$$
$$-\frac{A_{out}}{V_{cat}} h_{ext,cat} \left(T_{cat}(x,t) - T_{amb} \right) \tag{2}$$
$$-h_{int,cat} \; A_{geo} \left(T_{cat}(x,t) - T_g(x,t) \right) + Q_{cat,conv}(x,t),$$

where the first term is the heat conduction of the solid. The second term refers to the convective exchange between the ambient air and the solid. The third term couples (2) to (1) with the internal convection between the solid and the gas phases. $Q_{cat,conv}$ is the heat released by the conversion of pollutants and is detailed in the following section. The parameters of the model can be found in Table 1.
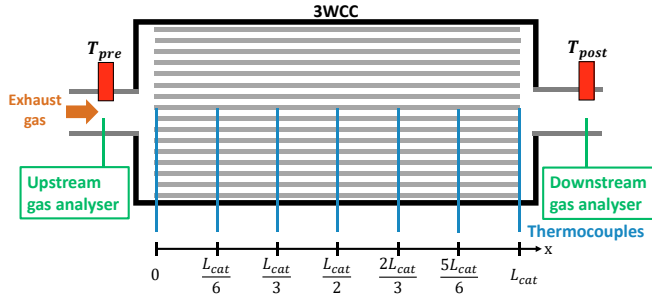
Fig. 3: Scheme of the sensors layout used in the experiments.

2.3. Conversion model

As explained in the introduction, the exothermic reactions caused by the conversions of pollutants are simplified by Michel et al. (2014):

$$Q_{cat,conv}(x,t) = \sum_{i=[CO,HC,NO_X]} \dot{m}_i(x,t) \frac{K_{i,react}}{V_{cat}} \eta_{i,conv}(x,t). \quad (3)$$

Contrary to Michel et al. (2014), the conversion of pollutants inside the 3WCC is not globally but locally considered. It leads to a spatial variation of the mass of pollutant:

$$\frac{\partial \dot{m}_i(x,t)}{\partial x} = -\dot{m}_i(x-dx,t) \frac{\eta_{i,conv}(x-dx,t)}{L_{cat}}. \quad (4)$$

The conversion efficiency is described as follows:

$$\eta_{i,conv}(x,t) = \frac{\dot{m}_{exh,max}}{\dot{m}_{exh}(t)} \frac{\eta_{i,conv,max}}{2} \\ \left(1 + \tanh\left(s_i\left(T_{cat}(x,t) - T_{i,LO}\right)\right)\right). \quad (5)$$

We assume that the 3WCC is sized to convert all the pollutants at maximum exhaust mass flow. Therefore, the time of residence in the catalytic converter is taken into account with the ratio of exhaust mass flow. The light-off temperature $T_{i,LO}$ corresponds to the catalytic temperature where the efficiency of conversion hits 50%.

2.4. Thermal model of Tpost

A thermocouple is placed downstream of the 3WCC to measure the gas temperature. However, heat transfers between the 3WCC's output and the thermal sensor need to be taken into account. Therefore, a simplified model of the gas temperature is developed, considering the pipe as a perfect heat exchanger:

$$m_{post} C_{post} \frac{\partial T_{post}(t)}{\partial t} = -h_{ext,post} S_{ext,post}\left(T_{post}(t) - T_{amb}\right) \\ + h_{int,post} S_{int,post}\left(T_g(x=L_{cat},t) - T_{post}(t)\right). \quad (6)$$

The first term is the internal convection between the gas coming out of the 3WCC and the pipe's wall. The second term is the external convection between the tube and the ambient air.
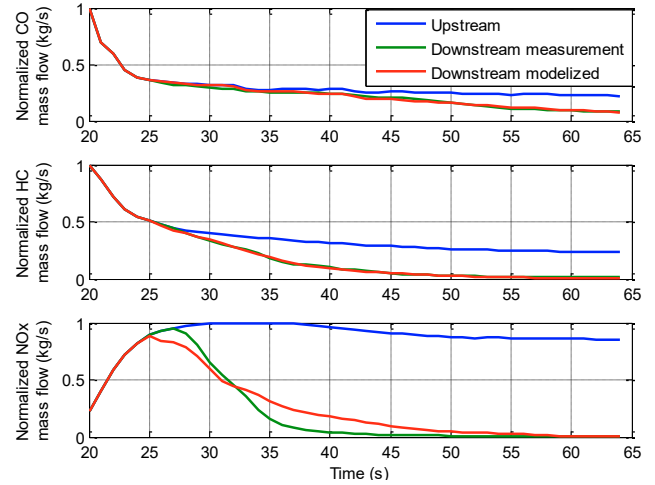

Fig. 4: Results of the identification of the conversion parameters.

3. MODEL'S IDENTIFICATION

The model previously presented contains multiple parameters that detail the exhaust gas, the catalytic converter, and the heat transfers. The geometry of the catalytic converter is considered as known, and the exhaust gas

parameters are taken from literature. Consequently, we need to identify parameters related to the thermal behaviour of the system and the conversion of pollutants.

In order to identify those parameters, the model is fitted to experimental data obtained on an engine test bed. The engine used for this work is a 3-cylinder indirect injection gasoline engine that is equipped with a close-coupled 3-way catalytic converter. As shown in Fig. 3, the catalytic converter is instrumented with thermocouples placed every 1/6 of the length so the entire solid temperature profile is known. Also, the gas temperatures upstream and downstream of the 3WCC are measured. Gas analysers are set on each side of the 3WCC to measure pollutant concentrations and are completed with an air mass flow sensor to measure the intake air mass flow.

3.1. Identification process

The model presented in part 2 contains 19 parameters that need to be identified. Considering this large number of parameters and in order to minimise dependencies, we proceed to identify the 9 parameters of (4) and (5) in a first phase. The values obtained from this phase will be used during the identification of the remaining parameters.

For each identification phase, a large number of parameters has to be identified. In order to reduce the time taken by that process, we use the Particle Swarm Optimization (PSO) algorithm of Kennedy et al. (1995) and adapted by Ebbesen et al. (2012) for the identification. This algorithm consists of minimizing a fitness function, such as a quadratic error between the measurement and the model, by searching for the best set of parameters for this function. In the first iteration, a defined number of random sets are tested. Then, each set of the next iteration is defined by a weighted function that takes
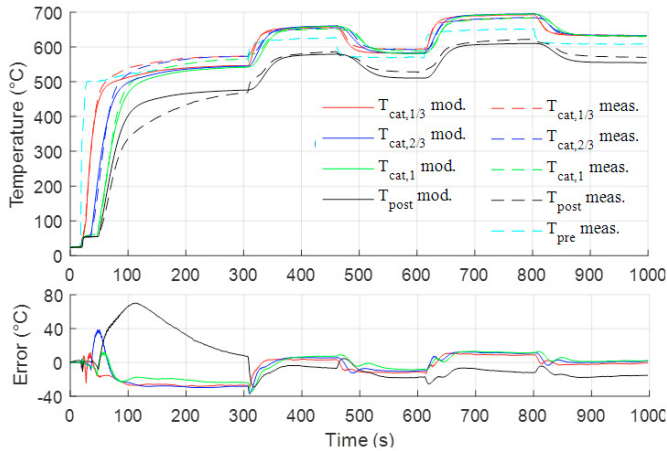
Fig. 5: Results of the identification with all the parameters.

into account its personal best position, the best overall position, the previous variation of the set and a random value. The algorithm goes on until the fitness function is sufficiently minimized, or until the maximum number of iterations is reached. By using this stochastic search method, we reduce the chance of encountering a local optimum of the fitness function.

3.2. Identification of the conversion parameters

The warm-up experiment shows an important variation a efficiency and therefore is used for the identification of the conversions parameters: $\eta_{i,conv,max}$, s_i, $T_{i,LO}$. The catalytic converter is set to 25°C at the start of the experiment. Then, the engine is turn on and regulated at a constant engine speed and torque. The measured temperatures of the catalyst converter are interpolated with respect to the longitudinal direction in order to obtain all the local temperatures and simulate the conversion rate profile of the 3WCC. Then, we use the upstream pollutant measurements given by the upstream gas analyser as input of the conversion model. Finally, the conversion parameters are identified from the minimization of the quadratic error of the mass of pollutants at the output of the catalytic converter between the model and the measurements given by the downstream gas analyser.

As shown in Fig. 4, CO and HC downstream mass flow are well modelled with a 5% quadratic error. However, NOₓ emissions are more difficult to reproduce here and the quadratic error rises to 9%. To explain this gap, while the hypothesis of a stoichiometric mixture is taken for the conversion model, a slightly rich exhaust gas is detected during the experiment due to combustion on cold conditions. Consequently, the rate of conversion for NOₓ can't be reproduced as well as for other pollutants. This issue could be resolved with a system that disconnect the after-treatment system from the engine during its cold phase and reconnect it once it is thermally stabilized.

3.3. Identification of the thermal model

The warm-up experiment is used again with the parameters found in the previous identifications. The last parameters are
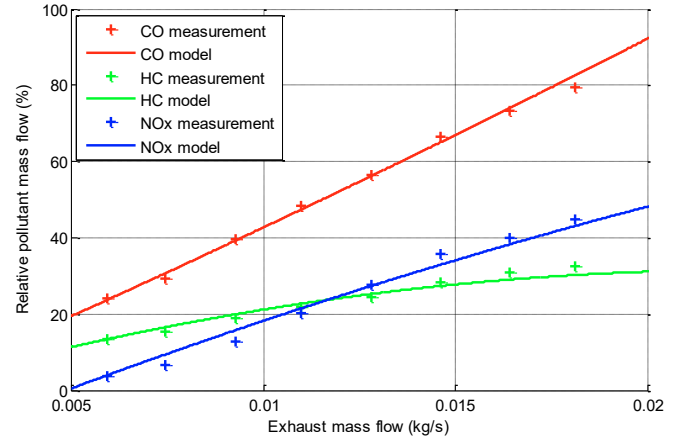

Fig. 6: Identification of the engine out pollutants model.

obtained by minimizing the quadratic error between the measured temperatures and the modelled ones. Then, the whole model is validated on different operating points as shown in Fig. 5. The temperatures inside the catalytic converter are identified with a maximum error of 40°C. However, the gas temperature downstream the catalytic converter has a maximum error of 70°C. The dynamic before 300 seconds is difficult to identify properly because $h_{int,cat}$ is identified as a constant value whereas it is dependent on $\dot{m}_{exh}$ and T_g. However, the model works well after 300 seconds with a less than 20°C error.

4. REAL-TIME ESTIMATION OF THE TEMPERATURE

In order to obtain a more accurate and real-time estimation of the temperature, we designed an EKF and implemented it on the test bed. Contrary to Utz et al. (2014), we do not use a measurement inside the 3WCC but a downstream gas temperature measurement designated as T_{post} in Fig. 3.

4.1. State-space representation

To solve computational and implementation issues, some assumptions are made to obtain the non-linear state space representation of the system. First of all, the hyperbolic tangent is linearized by a Taylor expansion of the first order and (5) becomes:

$$\eta_{i,conv}(x,t) = \frac{\dot{m}_{exh,max}}{\dot{m}_{exh}(t)} \frac{\eta_{i,conv,max}}{2} \left(1 + s_i \left(T_{cat}(x,t) - T_{i,LO}\right)\right). \quad (7)$$

Then an engine-out pollutant model, dependent on the engine speed and exhaust mass flow is created:

$$\dot{m}_{i=[CO,HC,NO_X]}(x=0,t) = f_i\left(\dot{m}_{exh}(t), \omega_e(t)\right). \quad (8)$$

For each engine speed, the three coefficients of a second order polynomial function f_i are identified by minimizing the quadratic error between the model and the measurement performed on the test bed (Fig. 6). To implement the estimator on the test bed, the previous model is discretized on three nodes in the catalytic converter. A Euler explicit

scheme is used for the space discretization. Therefore, we obtain the following states equations for each node:

$$\dot{T}_{g,\frac{1}{3}} = f_1\left(T_{pre}, T_{g,\frac{1}{3}}, T_{g,\frac{2}{3}}, T_{cat,\frac{1}{3}}, \dot{m}_{exh}, \omega_e\right), \tag{9}$$

$$\dot{T}_{cat,\frac{1}{3}} = f_2\left(T_{g,\frac{1}{3}}, T_{cat,\frac{1}{3}}, T_{cat,\frac{2}{3}}, T_{amb}, \dot{m}_{exh}, \omega_e\right), \tag{10}$$

$$\dot{T}_{g,\frac{2}{3}} = f_3\left(T_{g,\frac{1}{3}}, T_{g,\frac{2}{3}}, T_{g,\frac{3}{3}}, T_{cat,\frac{2}{3}}, \dot{m}_{exh}, \omega_e\right), \tag{11}$$

$$\dot{T}_{cat,\frac{2}{3}} = f_4\left(T_{g,\frac{2}{3}}, T_{cat,\left[\frac{1}{3}\frac{2}{3}\frac{3}{3}\right]}, T_{amb}, \dot{m}_{exh}, \omega_e\right), \tag{12}$$

$$\dot{T}_{g,\frac{3}{3}} = f_5\left(T_{g,\frac{2}{3}}, T_{g,\frac{3}{3}}, T_{post}, T_{cat,\frac{3}{3}}, \dot{m}_{exh}, \omega_e\right), \tag{13}$$

$$\dot{T}_{cat,\frac{3}{3}} = f_6\left(T_{g,\frac{3}{3}}, T_{cat,\left[\frac{1}{3}\frac{2}{3}\frac{3}{3}\right]}, T_{amb}, \dot{m}_{exh}, \omega_e\right), \tag{14}$$

$$\dot{T}_{post} = f_7\left(T_{post}, T_{g,\frac{3}{3}}, T_{amb}\right), \tag{15}$$

where f_{1-7} are non-linear functions described by (9) to (15). This set of equations is combined to build the non-linear state space representation of the system:

$$\begin{cases} \dot{\Theta}(t) = f_{1-7}(\Theta, U, t), \\ Y(t) = [0000001] \cdot \Theta, \end{cases} \tag{16}$$

with the states

$\Theta = \left[T_{g,1/3}, T_{cat,1/3}, T_{g,2/3}, T_{cat,2/3}, T_{g,3/3}, T_{cat,3/3}, T_{post}\right]^T$, the inputs

$U = \left[\dot{m}_{exh}, T_{pre}, T_{amb}\right]^T$ and T_{post} as output Y.

4.2. Extended Kalman Filter (EKF)

Since the system is non-linear, an EKF is used to estimate the temperature of the system. The EKF is composed of a prediction phase, using the previous estimation to project the model ($\hat{\Theta}_{pred,k+1}$) and the prediction's covariance ($P_{pred,k+1}$):

$$\hat{\Theta}_{pred,k+1} = \hat{\Theta}_{est,k} + f\left(\hat{\Theta}_{est,k}, U_k\right) dt, \tag{17}$$

$$P_{pred,k+1} = A_k P_{est,k} A_k^T + I W_d I^T, \tag{18}$$

where A_k is determined by the Jacobian around the operating point:

$$A_k = \begin{bmatrix} \dfrac{\partial f_1}{\partial \Theta_1} & \cdots & \dfrac{\partial f_1}{\partial \Theta_7} \\ \vdots & \ddots & \vdots \\ \dfrac{\partial f_7}{\partial \Theta_1} & \cdots & \dfrac{\partial f_7}{\partial \Theta_7} \end{bmatrix}_{\overline{\Theta_{est,k}}, \overline{U_k}}. \tag{19}$$
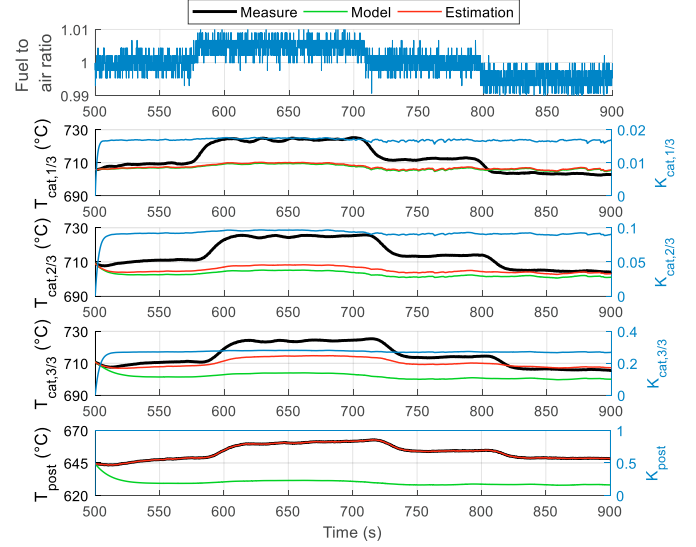

Fig. 7: Application of the observer with values of 100 on the diagonal of W_d.

The estimation phase corrects the prediction with the help of the measurement:

$$\hat{\Theta}_{est,k+1} = \hat{\Theta}_{pred,k+1} + K_{k+1}\left(Y_{k+1} - C_d \hat{\Theta}_{pred,k+1}\right), \tag{20}$$

with:

$$K_{k+1} = P_{pred,k+1} C_d^T\left(C_d P_{pred,k+1} C_d^T + V_d\right)^{-1}, \tag{21}$$

$$P_{est,k+1} = (I - K_{k+1} C_d) P_{pred,k+1}. \tag{22}$$

Uncertainties of the model and measurement are represented respectively by W_d and V_d while $C_d = [0\ 0\ 0\ 0\ 0\ 0\ 1]$. The objective of this EKF is to use the temperature measurement T_{post} to estimate correctly the 3WCC's temperature, taking into account the uncertainties of the models and the measurement.

4.3. Results

As explained previously, the EKF is dependent on two parameters for its estimation. In this study, the measure of T_{post} is considered to be reliable and is used to correct the model in order to give an estimation close to the measurement inside the 3WCC. By calculating the Allan variance, a two-sample variance that isolate the noise from the temperature drift of the thermocouple, V_d is deduced at 0.02. The uncertainty W_d needs to be tuned in order to obtain a good estimation.

4.3.1. W_d calibration

In order to evaluate the contribution of the observer, one can compare the estimation of the observer and the model against the experimental data. As a first test, we set a diagonal of 100 for W_d and see the influence of a 1% variation of the exhaust gas' fuel to air ratio on the 3WCC temperature. The results in
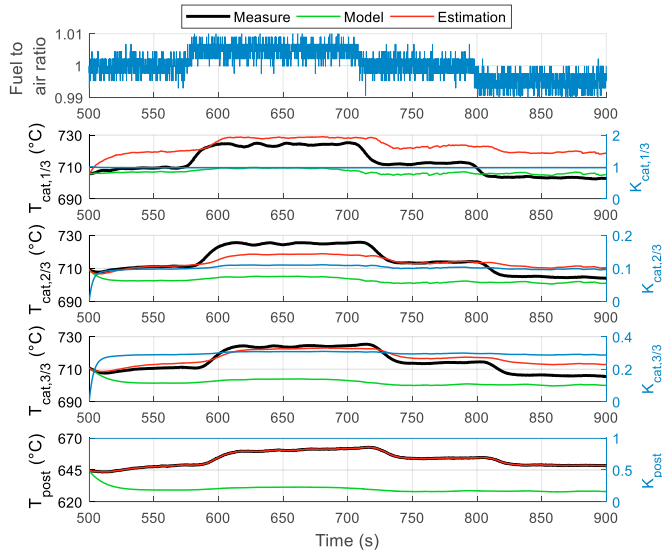
Fig. 8: Application of the observer with values of 100 on the diagonal of W_d and at $W_d(7,1)$.
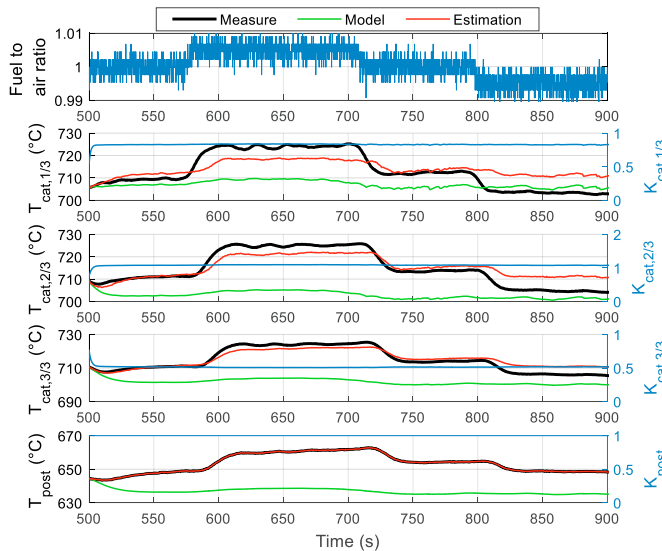

Fig. 9: Application of the observer after the identification of W_d.

Fig. 7 show that the value of K_{post} remains at one because the uncertainty level for the measurement is lower that the uncertainties of the model. $K_{cat,3/3}$ (Kalman gain for the estimation of $T_{cat,3/3}$) is in the order of 0.3 while $K_{cat,2/3}$ and $K_{cat,1/3}$ are lower and lower. Consequently, the estimations of $T_{cat,1/3}$ and $T_{cat,2/3}$ don't benefit from the improvement visible for $T_{cat,3/3}$. The low corrections on the states near the 3WCC's entry can be explained by the form of A_k that includes null elements on its superior triangle.

To reduce the estimation error for $T_{cat,1/3}$ and $T_{cat,2/3}$, the covariance between $T_{cat,1/3}$ and T_{post} is enabled (value 100) on W_d. As shown in Fig. 8, $K_{cat,1/3}$ becomes close to 1 and therefore and $T_{cat,1/3}$ is more sensitive to T_{post}'s variations.
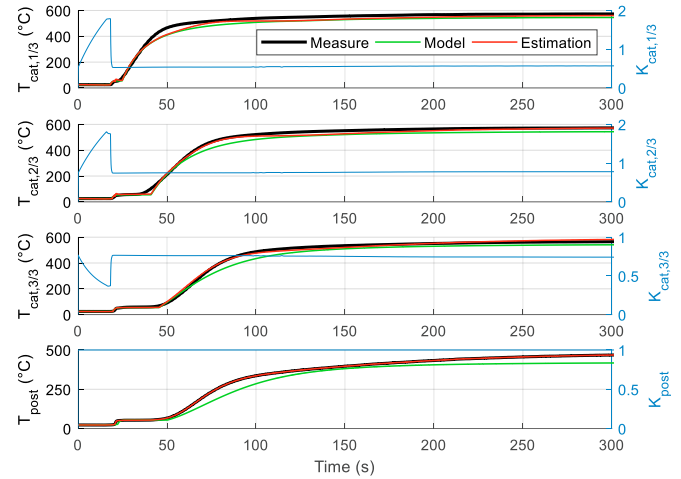

Fig. 10: Application of the estimator for the 3WCC's warm-up.
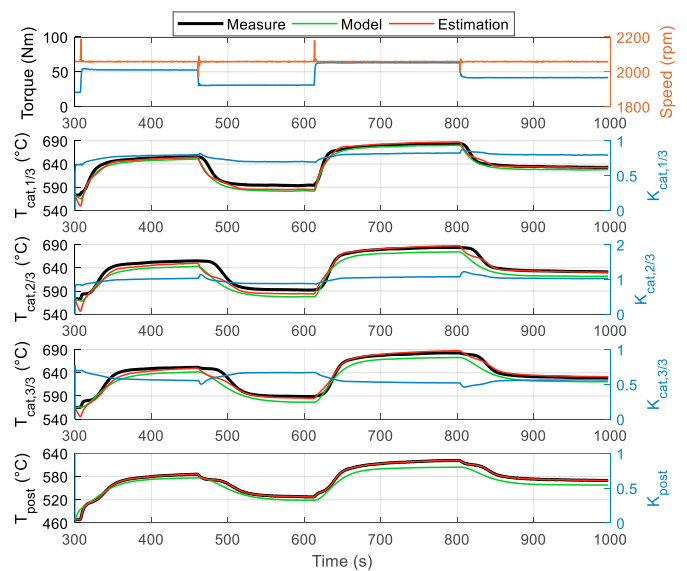

Fig. 11: Validation of the estimator with a variation of the engine's operating points.

Consequently, the estimation of $T_{cat,2/3}$ (that is partially deduced from $T_{cat,1/3}$) is also positively impacted by this new W_d.

This two examples show that the calibration of the 49 elements of W_d is complex. Therefore, the optimization Matlab function "fmincon" is applied in order to identify the elements of W_d that minimize the three estimation quadratic errors for $T_{cat,[1/3,2/3,3/3]}$. Fig. 9 and Table 2 show the results of the identification of W_d and demonstrate an error reduction from 40% to 80% compared to the model.

4.3.2. Validation of the observer

An interesting application of the observer is as a means of estimating important variations of internal temperature that can occur during the warm-up of the 3WCC (Fig. 10) and during a variation of operating point (Fig. 11). For the 3WCC

Table 2. Comparison of the quadratic errors (in °C) between the model and the observer

Experiment	Method	$T_{cat,1/3}$	$T_{cat,2/3}$	$T_{cat,3/3}$
Fuel to air ratio variation	Model	9.11	13.50	14.90
	Observer	5.38	3.87	2.87
Warm-up	Model	29.58	30.09	27.78
	Observer	19.42	10.62	13.94
Variation of operating point	Model	7.56	13.22	11.38
	Observer	6.12	8.13	5.83

warm-up (Fig. 10), the internal convection coefficient is reduced in order to keep the same error's sign between T_{post} and $T_{cat,[1/3,2/3,3/3]}$. Otherwise, the observer's correction has the wrong sign. In both cases, the observer allows a significant error reduction compared to the initial model (Table 2). The higher error for the warm-up must be put in the perspective of having a higher temperature variation than for the other cases. Despite the identification of the model on a different operating point, the observer is able to compensate for most of the static error. Moreover, it brings an improvement during the transitions of temperature. While the input delay of the system is not taken into account by the model, the observer gives the ability to correct the model in order to incorporate such phenomena. Consequently, this method is able to limit the complexity of the thermal model and increase the precision level of the estimation.

5. CONCLUSION

Tighter emissions standards lead to a better knowledge of the efficiency of the after-treatment systems and thus their temperatures. To improve the previous model and observer of temperature from the literature, we propose the addition of a local conversion term and use an observer with an easy to implement measurement downstream of the 3WCC. The model is identified with experimental data and compared to the observer. With the proper calibration of uncertainties, the observer is able to significantly improve the temperature estimations.

In the future, it would be interesting to improve the thermal model in order to have a better estimation during the warm-up phase. In addition, a similar observer, with a different exterior measurement and shorter time delay could be identified and applied. Other phenomena, like the relative oxygen level could be added to the model since the oxygen level capacity is also dependent on the temperature and is crucial during transient operation of the engine.

REFERENCES

Auckenthaler, T. S. (2005). Modelling and control of three-way catalytic converters. ETH Zurich.

Brandt, E. P., Wang, Y., & Grizzle, J. W. (2000). Dynamic modeling of a three-way catalyst for SI engine exhaust emission control. *IEEE Transactions on control systems technology*, *8*(5), 767-776.

Bresch-Pietri, D., Leroy, T., & Petit, N. (2013). Estimation of the distributed temperature of a SI engine catalyst for light-off strategy. In *European Control Conference* (pp. 1583-1590).Cioffi, V., Scala, S., & Sepe, E. (2001). Control oriented modeling of the exhaust gas after-treatment system. *TC*, *1*, V2.

Ebbesen, S., Kiwitz, P., & Guzzella, L. (2012, June). A generic particle swarm optimization Matlab function. In *American Control Conference (ACC), 2012* (pp. 1519-1524). IEEE.

Kennedy, R. (1995, November). J. and Eberhart, Particle swarm optimization. In *Proceedings of IEEE International Conference on Neural Networks IV, pages* (Vol. 1000).

Michel, P., Charlet, A., Colin, G., Chamaillard, Y., Bloch, G., & Nouillant, C. (2014, August). Catalytic converter modeling for optimal gasoline-HEV energy management. In *19th IFAC World Congress, IFAC'14* (pp. 6636-6641).

Michel, P., Charlet, A., Colin, G., Chamaillard, Y., Bloch, G., & Nouillant, C. (2015). Optimizing fuel consumption and pollutant emissions of gasoline-HEV with catalytic converter. *Control Engineering Practice*, *61*, 198-205.

Sabatini, S., Kil, I., Dekar, J., Hamilton, T., Wuttke, J., Smith, Hoffman M. A., & Onori, S. (2015). A new semi-empirical temperature model for the three-way catalytic converter. *IFAC-PapersOnLine*, *48*(15), 434-440.

Simon, A., Michel, P., Nelson-Gruel, D., Chamaillard, Y., & Nouillant, C. (2015, October). Gasoline-HEV equivalent consumption and pollutant minimization strategy. In *Vehicle Power and Propulsion Conference (VPPC), 2015 IEEE* (pp. 1-6). IEEE.

Utz, T., Fleck, C., Frauhammer, J., Seiler-Thull, D., & Kugi, A. (2014). Extended Kalman filter and adaptive backstepping for mean temperature control of a three-way catalytic converter. *International Journal of Robust and Nonlinear Control*, *24*(18), 3437-3453.